

# A LOW POWER, MICROVALVE-REGULATED DRUG DELIVERY SYSTEM USING A SI MICRO-SPRING PRESSURIZED BALLOON RESERVOIR

Allan T. Evans<sup>1</sup>, Jong M. Park<sup>1</sup>, Gregory F. Nellis<sup>2</sup>, Sanford A. Klein<sup>2</sup>, Jeffrey R. Feller<sup>3</sup>, Louis Salerno<sup>3</sup>, and Yogesh B. Gianchandani<sup>1</sup>

<sup>1</sup>Department of Electrical Engineering and Computer Science, University of Michigan, Ann Arbor

<sup>2</sup>Department of Mechanical Engineering, University of Wisconsin, Madison

<sup>3</sup>NASA Ames Research Center, Moffett Field, CA 94035

**ABSTRACT:** This paper reports on a drug delivery system that provides modulated delivery of liquid-phase chemicals. The device uses silicon torsion springs on a  $2 \times 3 \text{ cm}^2$  chip to pressurize a soft polymeric reservoir and regulate flow with a piezoelectrically actuated silicon microvalve that is  $1.5 \times 1.5 \times 1 \text{ cm}^3$ . Using the finished device, regulated diffusion of a fluorescent dye into agar gel was demonstrated. Fluid flow out of the  $500 \mu\text{L}$  reservoir could be regulated from 10-500  $\mu\text{L}/\text{min}$  with up to 80 kPa of delivery pressure. Typical regulation consumes  $0.136 \mu\text{W}$  of power. Analysis of the valve, reservoir springs, and a model based on pressure-enhanced diffusion are presented and are validated by experimental data.

**KEYWORDS:** Drug Delivery, Piezoelectric, Microvalve, Torsion Springs

## I. INTRODUCTION

Significant advances have been made for low power delivery of solid-phase drugs in recent years. For example, biodegradable polymers have been developed for implantable delivery [1]. For liquid-phase drugs, micropumps are used in delivering medication from a reservoir that is periodically refilled. They are generally larger in size, and they are often located outside of the body [2]. The existing pump systems present significant opportunity for miniaturization and power savings [3]. In this paper, we describe a valve-regulated system that uses a very low power architecture. One class of targets for this approach is intrathecal drugs such as morphine, pethidine, and epidural, but it may also be scaled to insulin (Table 1) [4].

The device operates by using a piezoelectric valve to regulate the flow from a pressurized elastic reservoir (Fig. 1). This type of device regulates flow in a much different manner than traditional pumps. The reservoir acts as a pressure source that, in conjunction with the target, creates a pressure gradient across the valve. Small total size and sufficient flow regulation can be achieved with a liquid reservoir that can generate relatively large backpressures. Reservoirs can be pressurized with motors, gas, or mechanical springs. To keep the device small, the passive pump/reservoir is created by using microfabricated silicon springs that press against a 4 mm diameter polyethylene

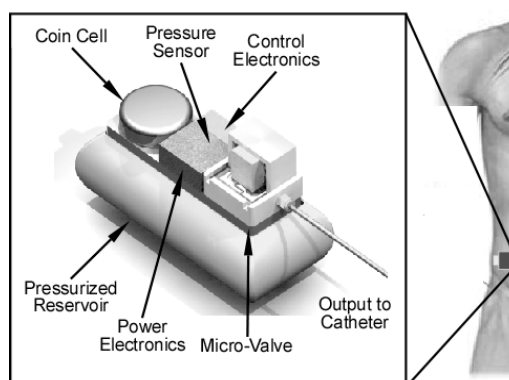


*Fig. 1: Proposed system schematic. Inset is a catheter connected, microvalve controlled, portable drug delivery system.*

terephthalate (PET) angioplasty balloon to pressurize the liquid. The reservoir has a total volume of  $502 \mu\text{L}$  when fully expanded.

The control valve actively regulates the flow of medication by changing the hydraulic resistance. Many microvalves have been previously reported [5-7]. This delivery application required that the chosen valve needed to optimize power consumption, force generation, maximum flow rate, and high pressure operation. A partially open piezoelectric valve that provides large operating pressures and requires minimal power is used [8]. In this paper, we evaluate the microvalve and pressurized reservoir.

## II. DEVICE CONCEPTS AND OPERATION

Designing the reservoir using traditional helical or leaf springs would require large, long devices because they generate force related to length and displacement. Torsion springs are used because they provide a compact alternative because torque is dependent upon the spring constant and the angle of deflection. Only

Table 1: Delivery rates for common medications

Drug	Normal Delivery Rate
Morphine	20 – 167 $\mu\text{L}/\text{min}$
Pethidine	10 – 250 $\mu\text{L}/\text{min}$
Epidural	0 – 200 $\mu\text{L}/\text{min}$
Insulin	2 – 350 $\mu\text{L}/\text{hr}$

the torsion spring constant and the arm length affect the final spring size. The reservoir is pressurized by 50 springs in parallel. The springs further from the outlet of the reservoir are stiffer than the springs near the outlet. This creates a gradient that empties the reservoir from the rear like a tube of toothpaste. The final serpentine torsion springs consist of bends that measured  $40\ \mu\text{m}$  deep,  $60\ \mu\text{m}$  wide, and  $150\ \mu\text{m}$  long. The average total spring length is  $3500\ \mu\text{m}$  on each side of the reservoir.

The valve operates by using a lead zirconate titanate (PZT) stack to press the silicon valve seat against a glass wafer. One design challenge in using a PZT actuator for the valve is that only a small stroke can be generated. This limits the flow modulation that can be achieved with a given inlet pressure. One way to reduce the hydraulic resistance, and thus the flow rate, is to increase the valve seat perimeter. This was done by making it serpentine. This increases the width of the flow channel across the valve seat from  $5\ \text{mm}$  to  $160\ \text{mm}$ , resulting in an increase in the maximum flow rate of almost two orders of magnitude.

### III. DEVICE FABRICATION

The microspring fabrication process uses a silicon-on-insulator (SOI) wafer which has an epitaxial layer, a buried oxide layer, and bulk wafer thicknesses of  $40\ \mu\text{m}$ ,  $0.5\ \mu\text{m}$ , and  $400\ \mu\text{m}$ , respectively (Fig. 2). The buried oxide layer provides an etch stop for deep reactive ion etching (DRIE), while the epitaxial layer provides a well-controlled spring thickness and provides bulk silicon properties. PECVD oxide is deposited on the front side of the wafer (Step 1). The oxide is then patterned by a plasma etch to define the torsion springs (Step 2). Both the photoresist and oxide act as one mask for a DRIE etch down to the buried oxide layer from the top side of the wafer. This defines the bulk silicon springs (Step 3). About  $5\ \mu\text{m}$  of PECVD oxide is deposited on the back side of the

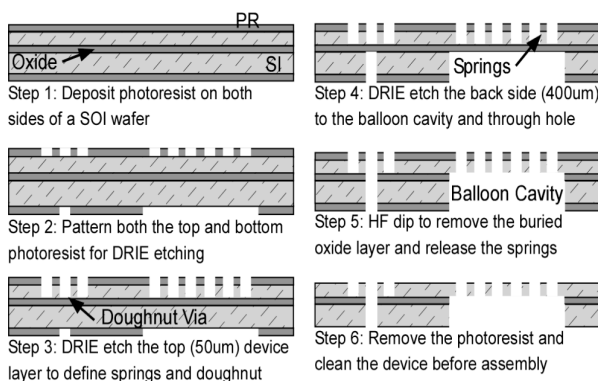


*Fig. 2: Silicon process: springs are formed on device layer of the wafer by a DRIE etch. The buried oxide layer acts as an etch stop for the cavity and HF dip removes the oxide layer to release the springs.*

wafer. The oxide is patterned by plasma etching to create backside windows underneath the springs. Next, the oxide and photoresist mask a  $400\ \mu\text{m}$  DRIE etch to the buried oxide layer (Step 4). Lastly, the wafer is etched in HF to remove the insulating and oxide masking layers and release the springs (Step 5).

As presented earlier [9], the microvalve process uses a SOI wafer and a glass wafer. Two DRIE etches are used to create a bossed membrane, and to define serpentine groove patterns in the valve seat. A glass wafer is recessed  $2\ \mu\text{m}$  to create a normally open flow channel. Inlet and outlet holes are HF wet etched, and the glass is anodically bonded to the processed silicon wafer (Fig. 3).

The reservoir is assembled from the silicon springs, a PET balloon, and a bulk plastic substrate. The torsion springs are aligned to the balloon, and the edges of the die are secured to the plastic base using epoxy. The PET tubing for the inlet and the outlet of the reservoir are connected to nozzles that interface between the reservoir and Tygon tubing (ID  $1.52\ \text{mm}$ ) used to interconnect the entire system. The finished valves are assembled from commercial PZT stacks, (Macor™) ceramic housing, and the microfabricated glass-silicon structure (Fig. 4). When actuated, the springs twist to generate torque (Fig. 5).

To create a normally-open valve with a consistent opening, the PZT stack is energized to  $30\ \text{V}$  during assembly. A ceramic header is machined and bonded to the top side of the valve using epoxy. The header acts as an interface between the glass inlet and outlet

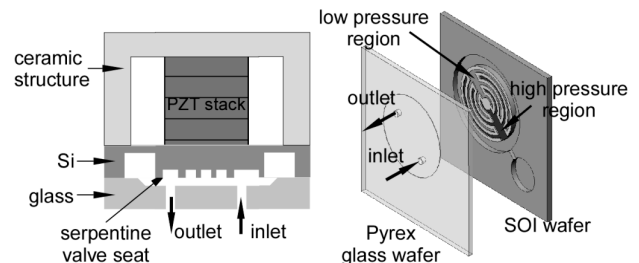


*Fig. 3: Valve cross-section, ceramic-PZT-Si-glass structure with 3-D visualization of valve membrane.*

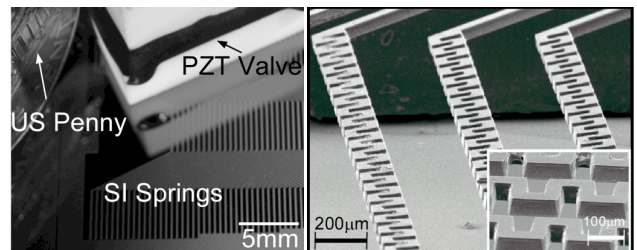


*Fig. 4: Picture of microvalve attached to the header, springs, and a US penny.*

*Fig. 5: SEM of the actuated silicon torsion springs. The twist can be clearly seen. Inset is a close up view.*

ports and standard 1/16" stainless steel piping. This piping is easily connected to the Tygon tubing and allows for an easily interconnected system.

#### IV. EXPERIMENTAL RESULTS

To characterize the springs, the reservoir was filled and resultant pressures were monitored. The gas pressure was increased and then held constant as the deflection of the valve was measured. The process was repeated until the balloon was filled. The reservoir was emptied and the process was repeated. Optical methods were used to measure the deflection of up to 4 mm as the reservoir was filled (Fig. 7). The spring deflection for various pressures (Fig. 8) was nonlinear, and typically required up to 80 kPa to fully fill the reservoir.

Many devices deliver medication through a catheter that then diffuses into subcutaneous fat or into cerebral tissue in the spine. To regulate medication delivered in this manner, a device has to be able to control diffusion into these tissues. To verify active control over diffusion, the entire system was filled with fluorescent dye and tested by regulating delivery into agar gel. Approximately 0.136  $\mu$ W of power consumption was measured by monitoring the actuation voltage and current during operation. This test setup demonstrates a wide diffusion range with varying control voltages (Fig 9). The use of a 26G asymmetric needle for constant depth resulted in the visible non-circular diffusion patterns.

A MatLab software analysis was conducted on diffusion image bisectors. The normalized fluorescent intensities for the various voltages over time (Fig. 10) further suggest that the valve regulated drug delivery device can actively control medication delivery. These results are used in a constant source diffusion model.

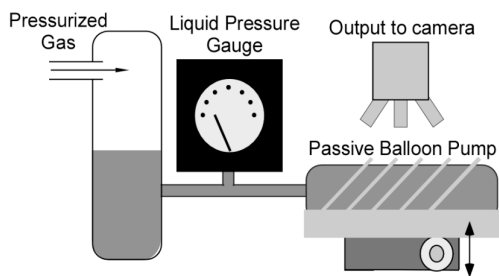


Fig. 6: Setup to measure deflection of springs using z-axis focal adjustment.



Fig. 7: Actuated silicon torsion springs with a PET angioplasty balloon acting as a liquid reservoir.

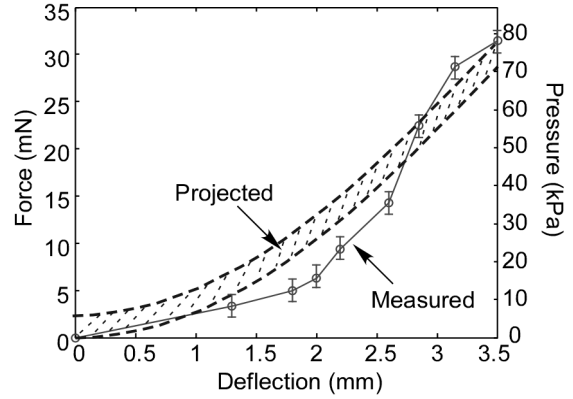


Fig. 8: Measured and predicted z-axis spring deflection from the assembled balloon reservoir with typical resultant spring forces and liquid pressures.

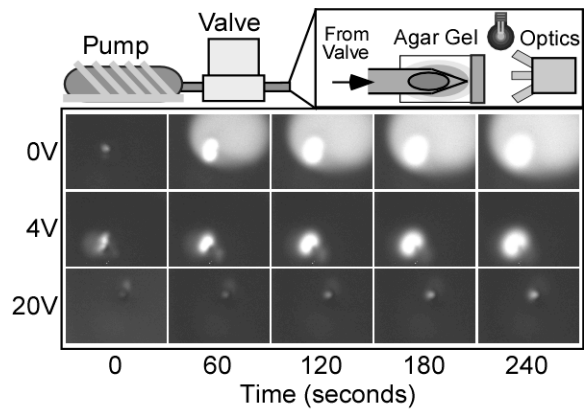


Fig. 9: Test using microvalve to regulate fluorescent diffusion from a spring pump into agar gel. The test setup is on top and typical fluorescent images taken for different valve actuation voltages are shown over time.

#### V. ANALYSIS

ANSYS simulation results were used to create an analytical MatLab model of deflection versus the z-axis force generated. The predicted results from simulation are plotted against the actual measured results of spring pressure and deflection with the varying widths of the unfilled balloon (Fig. 8). The variation from simulation is likely due to the balloon folds interacting with the springs.

Constant-source diffusion models based on Fick's law (Eqn. 1) were mapped to intensity at various modulation levels presented by the valve (Fig.10).

$$N(x,t) = N_0 * \text{erfc}\left(\frac{x}{2\sqrt{Dt}}\right) \quad (1)$$

The model assumes the needle acts like a constant source. Matlab software was used to determine the  $Dt$  products for every point independently by using the constant source diffusion model and a least squares fit of the diffusion images (Fig.11). If diffusion is

Fickian, these constants should form a line because the diffusion constant should be the same for a given voltage, and the points should be this constant multiplied by time with an initial offset. The very close linear fit of these independently determined constants lends credence to the analytical model. The determined diffusion constants were inserted into the constant source model, and it was then used to predict time-based diffusion distances for particular fluorescent concentrations across actuation voltages. This model makes several assumptions for simplification, but its close accuracy suggests that this valve can be used to achieve active control over diffusion.

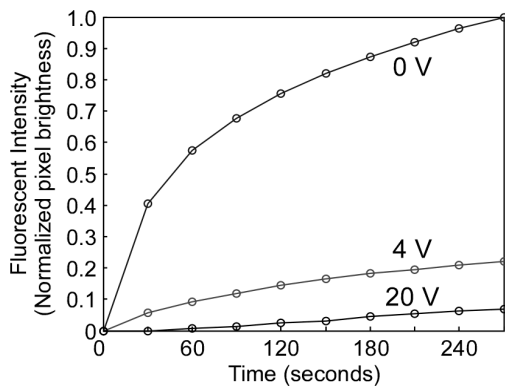


Fig. 10: Normalized output of total intensity of diffusion into agar for actuation voltages over time.

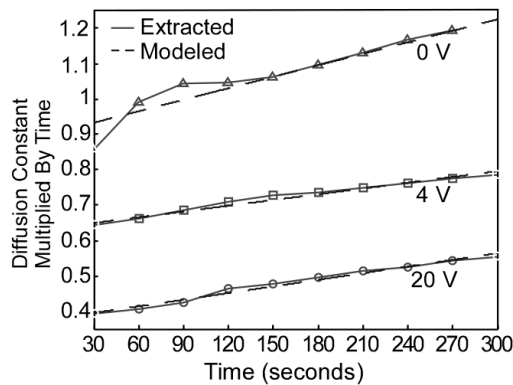


Fig. 11: Extracted  $Dt$  values for infinite source diffusion with modeled values showing close fit.

## VI. CONCLUSION

A PZT valve has been integrated with a pressurized reservoir to actively control aqueous flow and diffusion into agar gel. The current valve is suited to regulating high flow drugs that require 10-500  $\mu\text{L}/\text{min}$ . A reservoir was fabricated using bulk silicon to form torsion springs that applied pressurizing force on a PET balloon of up to 80 kPa. Lastly, the system was integrated, and diffusion into agar gel was

controlled. The diffusion was modeled considering the needle as a constant source. The close match between the experimental results and the diffusion model demonstrates active control over diffusion using a hybrid device. The results suggest that this device could be used to regulate the delivery of medication into subcutaneous fat or cerebral tissue. Preliminary results indicate that the proposed device could provide a promising drug delivery tool that would allow active control over the medication rate while consuming less than 1  $\mu\text{W}$  of power. The device could be programmed to operate closed loop and deliver medication in bolus injection, diffusion at a constant rate over several days, or a combination of both. This valve based device will consume less power and could be made smaller than current active pumps.

## References:

- [1] A.C.R. Grayson, I.S. Choi, B.M. Tyler, P.P. Wang, H. Brem, M.J. Cima, and R. Langer, "Multi-Pulse Drug Delivery from a Resorbable Polymeric Microchip Device" *Nature Materials*, 2(11), pp. 767-72, 2003
- [2] G.-H. Feng and E.S. Kim, "Piezoelectrically Actuated Dome-Shaped Diaphragm Micropump," *J. Microelectromech. Sys.*, 13(2), pp. 192-9, 2005
- [3] B. Ziaie, et. al., "Hard and Soft Micromachining for BioMEMS: Review of Techniques and Examples of Applications in Microfluidics and Drug Delivery," *Advanced Drug Delivery Reviews*, 56(2), pp. 145-72, 2004
- [4] L. Visser, "Epidural Anaesthesia," *Update in Anesthesia*, Issue 13, Article 11, 2001, pp. 1-4
- [5] M.A. Huff, J.R. Gilbert, and M.A. Schmidt, "Flow Characteristics of a Pressure-Balanced Microvalve," *Transducers '93*, Yokohama, Japan, 1993, pp. 98-101
- [6] C. Lee, E.H. Yang, S.M. Saeidi, and J.M. Khodadadi, "Fabrication, Characterization, and Computational Modeling of a Piezoelectrically Actuated Microvalve for Liquid Flow Control," *J. Microelectromech. Sys.*, 15(3), pp. 686-96, 2006
- [7] N. Vandelli, et. al., "Development of a MEMS Microvalve Array for Fluid Flow Control," *J. Microelectromech. Sys.*, 7(4), pp. 395-403, 1998
- [8] J.M. Park, et. al., "A Piezoelectric Microvalve with Integrated Sensors for Cryogenic Applications," *MEMS '07*, Kobe, Japan, Jan. 2007, pp. 647-50
- [9] A. Brask, et. al., "A Novel Electro-Osmotic Pump Design for Nonconducting Liquids: Theoretical Analysis of Flow Rate-Pressure Characteristics and Stability," *Journal of Micromechanics and Microengineering*, 15(4), pp. 883-91, 2005